Supplemental Table of Contents

MATERIALS AND METHODS

Human Veins and AVFs

Paraffin-embedded cross-sections of pre-access veins (N=20, 10 matured and 10 failed after AVF creation) from patients who received a planned two-stage upper arm AVF at Jackson Memorial Hospital or the University of Miami (UM) were randomly selected from the UM Vascular Biobank. In addition, 18 independent AVF specimens (8 matured and 10 failed) preserved in *RNAlater* (Qiagen) and collected at the time of second-stage surgery were randomly obtained from the biorepository. All AVFs were created by a single vascular surgeon (M.T.). Anatomic non-maturation was defined as an AVF that never achieved an internal diameter ≥ 6 mm. The time from access creation to second-stage surgery was similar between AVFs that matured and those that failed (74.4 ± 27.1 vs. 66.7 ± 28.5 days, respectively; P=0.57), and both subgroups were comparable in terms of demographics and comorbidities. The second-stage surgery consisted of a standard AVF transposition for AVFs that matured or a salvage procedure (short transposition, ligation, or AVG extension) for those that failed. Enrolled patients were consented before sample collection at the corresponding surgeries. The study was performed according to the ethical principles of the Declaration of Helsinki and regulatory requirements at both institutions. The ethics committee and Institutional Review Board at the University of Miami approved the study.

Rat model of AVF maturation

Sprague Dawley rats (280-320 grams) were purchased from Envigo (Indianapolis, IN). AVFs were created by an end-to-side anastomosis of the epigastric

vein to the nearby femoral artery (1). Ninety-six rats of both sexes were randomly allocated to experimental groups. Molecular analysis of AVFs was performed at 0, 5, 20, and 33 days post-surgery (n=18). For systemic drug administration, rats were given a daily intraperitoneal injection of BAPN (100 mg/kg; Sigma-Aldrich, St. Louis, MO) (n=21) or PBS (vehicle, n=21) on days -2 to 21 post surgery. For local delivery, scaffolds with BAPN (n=18) or PBS (n=18) were wrapped around the epigastric vein immediately after AVF creation. Flow was measured using a flowmeter (Transonic Systems Inc., Ithaca, NY) prior to AVF harvesting at day 21. Rats were euthanized with isoflurane, after which AVFs were removed and placed in ice-cold normal saline for pressure myography, *RNAlater* for qRT-PCR, formalin for histology, or liquid nitrogen for collagen crosslinking analyses. The overall attrition rate was 4.2%, including 3 animals with postsurgical complications and one animal excluded due to technical reasons (see below).

Two out of the 42 rats used for systemic BAPN/vehicle injections were excluded due to complications with surgical sutures. From the remaining 40, 11 were used for intraoperative flow measurements followed by myography (3 males [M] and 3 females [F] in the vehicle group, 3M and 2F in the BAPN arm), 18 independent animals were used to measure fibrosis (5M and 4F in both experimental arms), and 11 independent rats were used for mass spectrometry (3M and 3F in the vehicle group, 2M and 3F in the BAPN arm).

One rat from the 36 included in the scaffold experiments was euthanized due to excessive postoperative bleeding. From the remaining 35, 11 were used for intraoperative flow measurements (3M and 2F in the vehicle group, 3M and 3F in the BAPN arm). One additional AVF in the vehicle arm was damaged during flow evaluation

and had to be excluded from the subsequent myography experiments. The final set for myography consisted of 2M and 2F in the vehicle arm, and the remaining 3M and 3F in the BAPN group). Eleven independent rats were used to measure fibrosis (2M and 3F in the vehicle group, 3M and 3F in the BAPN arm), and 12 more for mass spectrometry (3M and 3F in both experimental arms).

We did not suffer any attrition in the group of 18 rats used for molecular analyses. The four time points when gene expression was measured (0, 5, 20, and 33 days) included similar numbers of male and female animals: 2M and 1F at time zero, 3M and 3F at 5d, 3M and 3F at 20d, and 2M and 1F at 33d.

Scaffold fabrication and characterization

Scaffolds were fabricated using an electrospinning apparatus under the direction of F.M.A. Ester-terminated PLGA (Resomer® RG 504) was purchased from Sigma-Aldrich. PLGA (15% w/v) and drug (10% w/w PLGA) were dissolved in hexafluoroisopropyl alcohol and stirred overnight. PLGA solutions with and without drug were loaded into a 3 mL syringe attached to a blunt 22G stainless steel needle. A 20-kV voltage was applied to the needle. Flow was maintained at 2.0 mL/h using an Aladdin Single-Syringe Pump (World Precision Instruments, Sarasota, FL). Nanofibers were deposited on an aluminum-wrapped collector located 13 cm from the needle tip. Scaffolds were dried overnight in a fume hood to remove any residual solvent. Fiber architecture was analyzed using scanning electron microscopy (SEM) (JEOL Ltd., Tokyo, Japan) after gold sputter-coating. Fiber diameter was determined in ImageJ

(National Institutes of Health, Bethesda, MD) by adding scale bars to the width of randomly selected fibers before averaging. For degradation, pre-weighed sections of PLGA scaffolds were placed in 1.5 mL of PBS and incubated in a water bath at 37°C. Scaffolds were then removed from the PBS, lyophilized, and weighed, before incubating in fresh PBS again until the next time point. The “old” PBS was stored for mass spectrometry (MS). Cumulative BAPN release was determined in tandem with degradation experiments. Percent release was calculated as the ratio of BAPN in the supernatant to the initial amount of BAPN in the PLGA scaffold.

Mass spectrometry

Cumulative BAPN release was quantified with a direct infusion/ triple quadrupole mass spectrometer (TSQ)(2) configured in positive mode, 42 eV collision energy, [10.000-150.000 m/z] scan range, and parent-ion scan mode. Stock solutions of BAPN (1 mg/mL) and aminoacetonitrile internal standards (IS; 1 mg/mL) were prepared in methanol to establish the Internal Response Factor (IRF), (Equation I). After calculating the IRF, the Amount Specific Compound (SC) of BAPN (m/z=71.42) was determined in relation to the IS (m/z=57.47) at different time points over 60 days (Equation II).

$$Internal\ Response\ Factor = \frac{Intensity_{IS} * Amount_{SC}}{Amount_{IS} * Intensity_{SC}} \quad \text{(I)}$$

$$Amount\ Specific\ Compound = \frac{Amount_{IS} * Intensity_{SC} * IRF_{SC}}{Intensity_{IS}} \quad \text{(II)}$$

Immature (hydroxylysinonorleucine [HLNL], dihydroxylysinonorleucine [DHLNL]) and mature crosslinks (pyridinoline [PYD], deoxypyridinoline [DPD]) were quantified as previously described.(3) Briefly, human and rat AVF tissues were lyophilized overnight, reduced with sodium borohydride ($NaBH_4$) in NaOH, and hydrolyzed overnight with 6N HCl. Samples were lyophilized again and injected (5 µL) into an Acclaim™ Polar Advantage II LC reverse-phase column (Thermo Scientific™). MS was performed with positive electrospray ionization (ESI) with parameters and MRM transitions optimized for immature and mature crosslinks detection.(3) Crosslinks were quantified using the ratio of peak area of epinephrine to pyridoxine as IS. The calibration curves for HLNL, DHLNL, PYD, DPD, and hydroxyproline were established through a linear least-squares regression with a weighing factor of $1/C^2$. Immature and mature crosslinking density is expressed as the amounts of crosslinks per mg of dry weight of tissue.

Pressure myography

Rat AVFs were collected and cleaned of fat at 21 days post-surgery. The proximal and distal segment of the AVF were placed on a pair of steel cannulas (outer diameter: 900 or 1200 µm, depending on fistula size) of a pressure myograph system, DMT Model 110P (Danish Myo Technology, Ann Arbor, MI) and secured with surgical nylon sutures. After the distal segment of the artery was secured, and the vessel length adjusted to eliminate stretch, the intraluminal pressure was raised to 70 mmHg. The mounted vessels were equilibrated for 30 min at 37°C in calcium-free PSS gassed with a mixture of 95% O_2 and 5% CO_2, before reducing the intraluminal pressure to 3 mmHg. To obtain the pressure-diameter curve, the internal and external diameters were

measured while increasing intraluminal pressure in 10 mmHg steps between 3 and 130 mmHg. The diameters were recorded using the DMT MyoView 4 software (Danish Myo Technology). Distensibility was calculated as % deformation at increasing pressures with respect to the external diameter at 3 mmHg. The circumferential wall strain and stress and incremental elastic modulus (E_{inc}) were calculated as previously described.(4)

Immunohistochemistry

Paraffin-embedded rat AVFs were stained with Masson's trichrome to quantify wall fibrosis. Percent area of fibrosis was calculated in ImageJ using color thresholding. Briefly, images were converted to RGB format and color thresholds on the blue channel were used to segment the blue (collagen) from the red/pink (cells) staining.

For staining of LOX in human and rat AVFs, cross-sections were rehydrated by serially immersing them in xylene, alcohol, and water. Antigen retrieval for LOX staining was performed by boiling slides in 10 mM citrate buffer (pH 6.0) for 20 minutes. Antigen retrieval for elastin was done using proteinase K digestion for 10 minutes at 37°C. Next, sections were blocked for 20 minutes with Tris–Borate saline supplemented with 15% fetal bovine serum (FBS), followed by 3% hydrogen peroxide. Veins and AVFs were incubated with either anti-LOX polyclonal antibody at room temperature for 1 hour (Cat# ab31238, 1:200, Abcam, Cambridge, UK) or anti-elastin polyclonal antibody (Cat# ab23748, 1:200, Abcam) overnight. Bound antibodies were detected using the Dako Universal Link kit (Agilent, Santa Clara, CA), and color was developed with the Dako DAB+ Substrate Chromogen System (Agilent). Nuclei were counterstained with Meyer's

hematoxylin and mounted in Entellan (Sigma-Aldrich). Images were acquired using a VisionTek DM01 digital microscope (Sakura Finetek, Torrance, CA). Operators blinded to the clinical data performed digital processing of images.

Gene expression

Gene expression of Lox and LoxL genes was measured in rat AVFs harvested 5 days after surgery. For ECM genes and remodeling factors, tissues were collected at days 5, 20, and 33 after surgery. Samples were immediately stored in *RNAlater* at −80°C. Total RNA was isolated and reverse-transcribed as previously described.(5) Changes in gene expression were assessed using the following TaqMan Gene Expression Assays (Applied Biosystems, Waltham, MA): *Col1a1,* Rn01463848_m1*; Col3a1,* Rn01437681_m1*; Col5a1,* Rn00593170_m1*; Eln,* Rn01499782_m1*; Fbln5,* Rn00569712_m1*; Fgfr2,* Rn01269940_m1*; Fn1,* Rn00569575_m1*; Gapdh,* Rn99999916_s1*; Lox,* Rn01491829_m1*; Loxl1,* Rn01418038_m1*; Loxl2,* Rn01466080_m1*; Loxl3,* Rn01765241_m1*; Loxl4,* Rn01410872_m1*; Mmp2,* Rn01538170_m1*; Mmp9,* Rn00579162_m1*; Timp1,* Rn00587558_m1*; Timp2,* Rn00573232_m1*; and Timp4,* Rn01459160_m1*.* Real-time PCR was performed on an ABI Prism 7500 Fast Real-Time PCR System (96-well plate; Applied Biosystems). Relative gene expression was determined using the ΔΔCT method.(6) Gene expression was normalized with respect to GAPDH and expressed as fold change vs. the contralateral vein at the time of AVF creation.

Statistics

Statistical analyses were performed using GraphPad Prism version 8 for Windows (GraphPad Software, San Diego, CA). Normally distributed data were compared using unpaired t-tests with Welch's correction and expressed as mean ± standard deviation (or mean ± standard error of the mean [SEM] where indicated in figures). Non-normally distributed data were compared using the Mann-Whitney test and expressed as median and interquartile range (IQR). A P value < 0.05 was considered significant.

REFERENCES

1. Globerman AS, Chaouat M, Shlomai Z, Galun E, Zeira E, Zamir G: Efficient transgene expression from naked DNA delivered into an arterio-venous fistula model for kidney dialysis. *J Gene Med,* 13**:** 611-621, 2011 10.1002/jgm.1615
2. Machon C, Le Calve B, Coste S, Riviere M, Payen L, Bernard D, Guitton J: Quantification of beta-aminopropionitrile, an inhibitor of lysyl oxidase activity, in plasma and tumor of mice by liquid chromatography tandem mass spectrometry. *Biomed Chromatogr,* 28**:** 1017-1023, 2014 10.1002/bmc.3110
3. Hernandez DR, Del Carmen Piqueras M, Macias AE, Martinez L, Vazquez-Padron R, Bhattacharya SK: Immature and Mature Collagen Crosslinks Quantification Using High-Performance Liquid Chromatography and High-Resolution Mass Spectrometry in Orbitrap. *Methods Mol Biol,* 1996**:** 101-111, 2019 10.1007/978-1-4939-9488-5_10
4. Briones AM, Salaices M, Vila E: Mechanisms underlying hypertrophic remodeling and increased stiffness of mesenteric resistance arteries from aged rats. *J Gerontol A Biol Sci Med Sci,* 62**:** 696-706, 2007 10.1093/gerona/62.7.696
5. Martinez L, Tabbara M, Duque JC, Selman G, Falcon NS, Paez A, Griswold AJ, Ramos-Echazabal G, Hernandez DR, Velazquez OC, Salman LH, Vazquez-Padron RI: Transcriptomics of Human Arteriovenous Fistula Failure: Genes Associated With Nonmaturation. *Am J Kidney Dis,* 74**:** 73-81, 2019 10.1053/j.ajkd.2018.12.035
6. Livak KJ, Schmittgen TD: Analysis of relative gene expression data using real-time quantitative PCR and the 2(-Delta Delta C(T)) Method. *Methods,* 25**:** 402-408, 2001 10.1006/meth.2001.1262

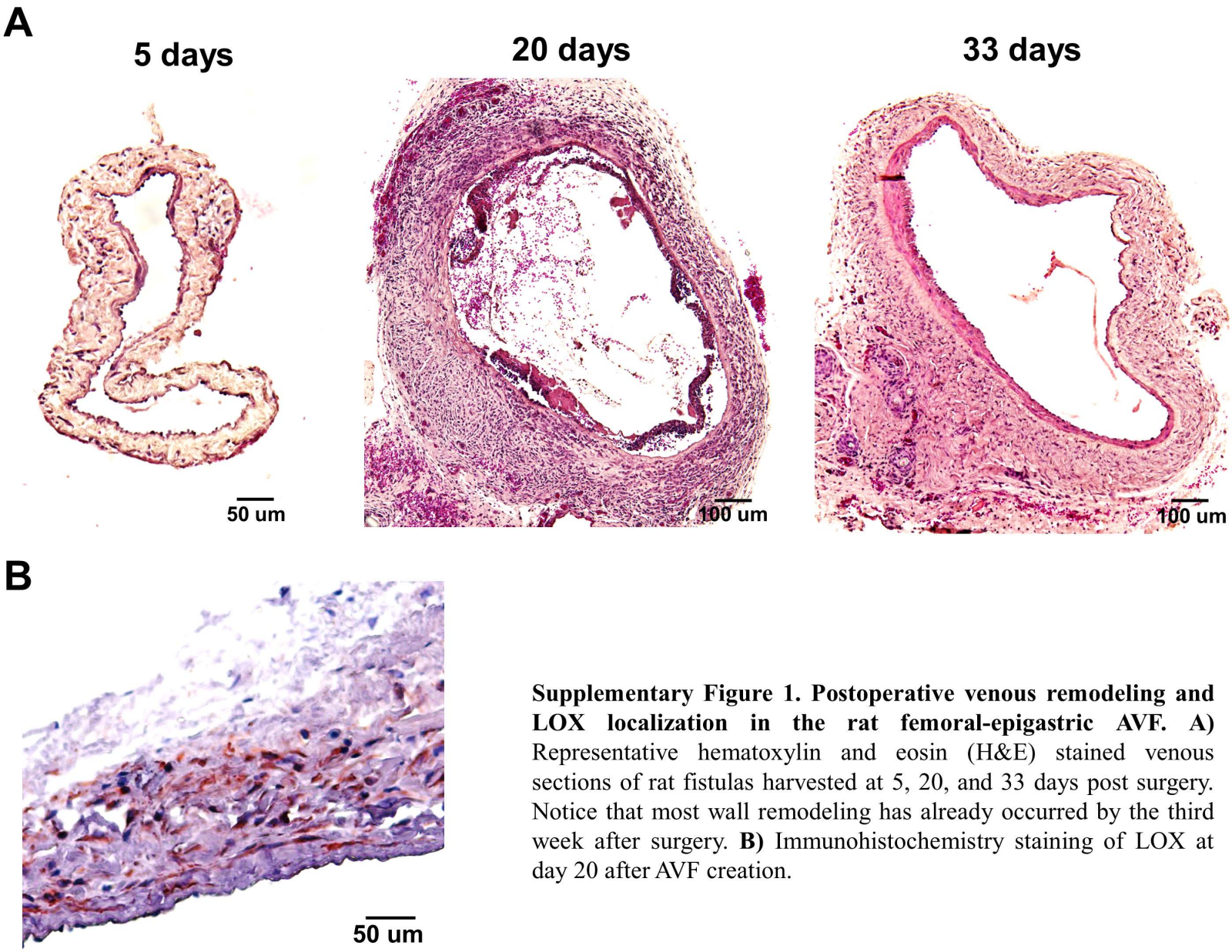

Supplementary Figure 1. Postoperative venous remodeling and LOX localization in the rat femoral-epigastric AVF. A) Representative hematoxylin and eosin (H&E) stained venous sections of rat fistulas harvested at 5, 20, and 33 days post surgery. Notice that most wall remodeling has already occurred by the third week after surgery. **B)** Immunohistochemistry staining of LOX at day 20 after AVF creation.

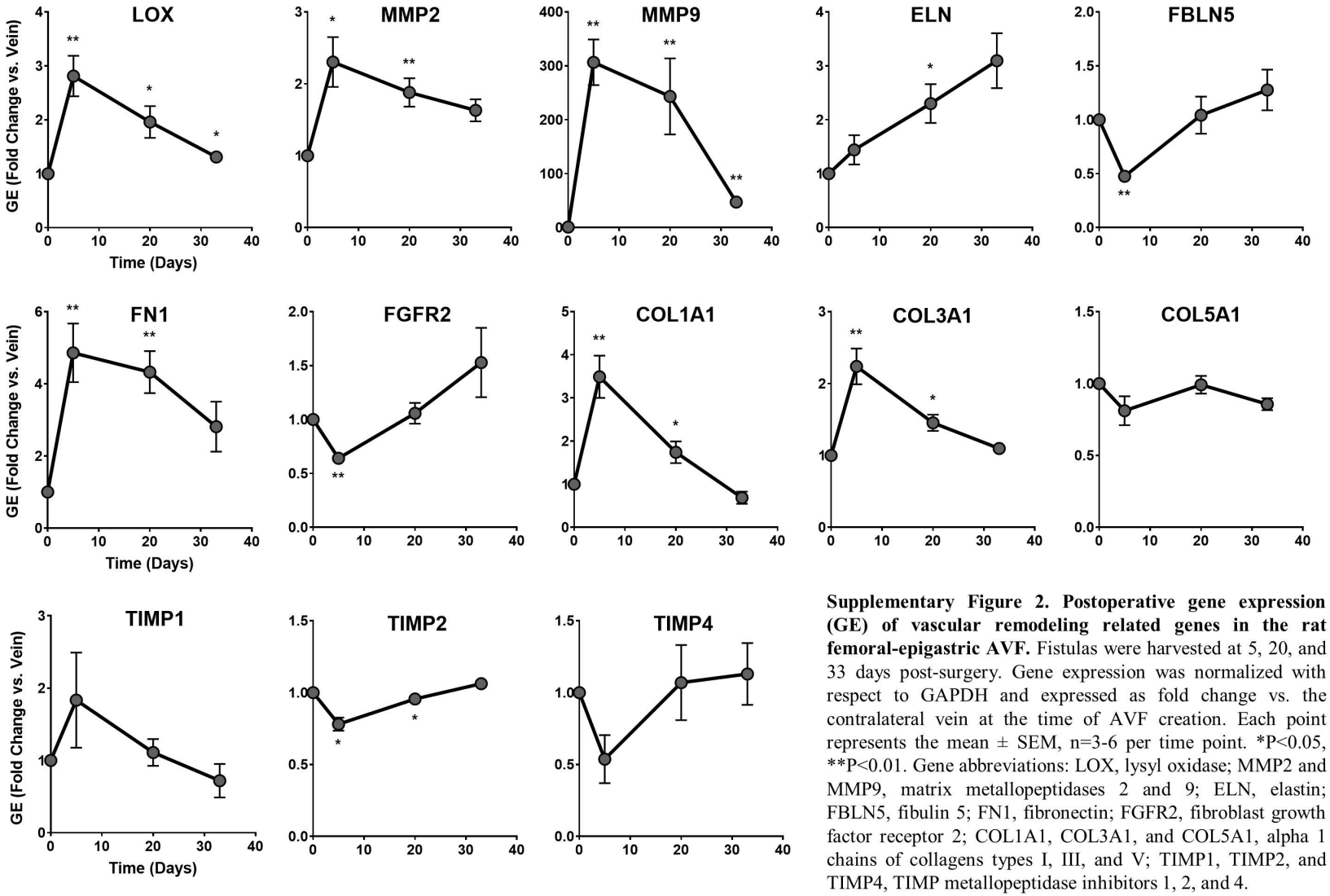

Supplementary Figure 2. Postoperative gene expression (GE) of vascular remodeling related genes in the rat femoral-epigastric AVF. Fistulas were harvested at 5, 20, and 33 days post-surgery. Gene expression was normalized with respect to GAPDH and expressed as fold change vs. the contralateral vein at the time of AVF creation. Each point represents the mean ± SEM, n=3-6 per time point. *P<0.05, **P<0.01. Gene abbreviations: LOX, lysyl oxidase; MMP2 and MMP9, matrix metallopeptidases 2 and 9; ELN, elastin; FBLN5, fibulin 5; FN1, fibronectin; FGFR2, fibroblast growth factor receptor 2; COL1A1, COL3A1, and COL5A1, alpha 1 chains of collagens types I, III, and V; TIMP1, TIMP2, and TIMP4, TIMP metallopeptidase inhibitors 1, 2, and 4.

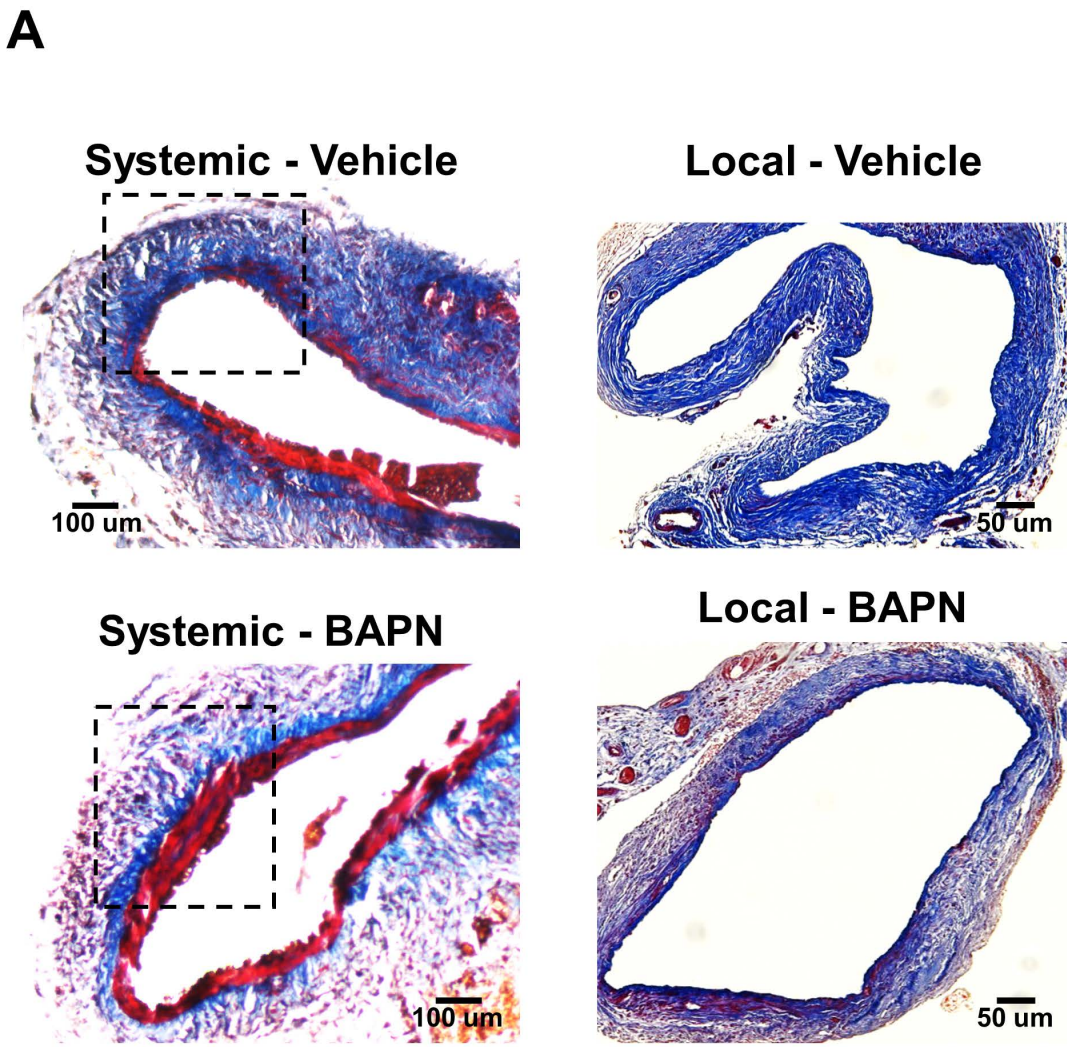

Supplementary Figure 3. Fibrosis and wall thickness in BAPN-treated and control AVFs. A) Representative Trichrome stained venous sections of rat AVFs harvested at 21 days post surgery. Animals were treated with systemic or local (via scaffold) BAPN or vehicle. Quantifications are presented in Figures 3C and 4D. Dashed boxes indicate areas magnified in Figure 3C. **B)** Average wall thickness in the four treatment groups. Data are presented as mean ± SEM (n=5-9 per group). **P<0.01, ***P<0.001

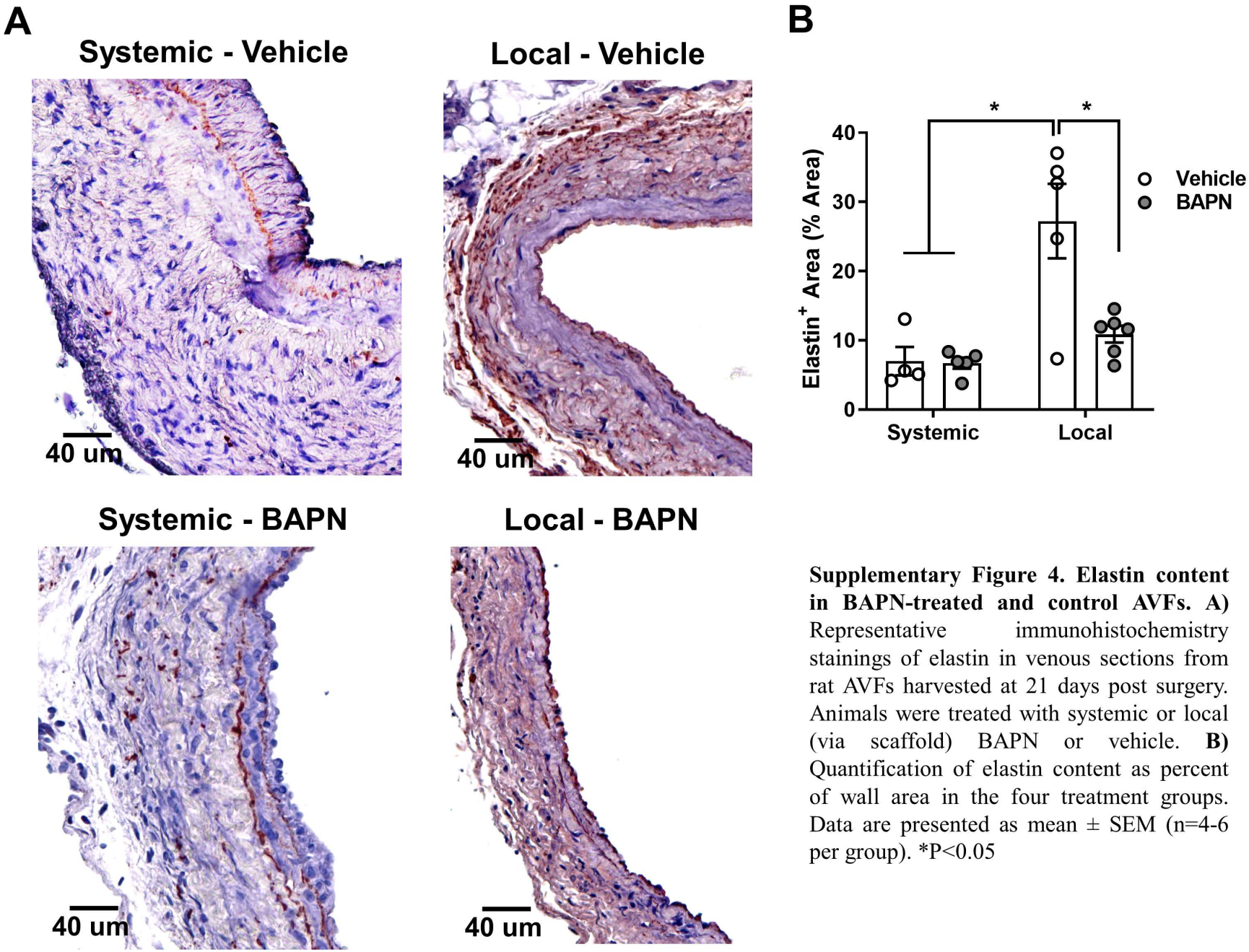

Supplementary Figure 4. Elastin content in BAPN-treated and control AVFs. A) Representative immunohistochemistry stainings of elastin in venous sections from rat AVFs harvested at 21 days post surgery. Animals were treated with systemic or local (via scaffold) BAPN or vehicle. **B)** Quantification of elastin content as percent of wall area in the four treatment groups. Data are presented as mean ± SEM (n=4-6 per group). *P<0.05

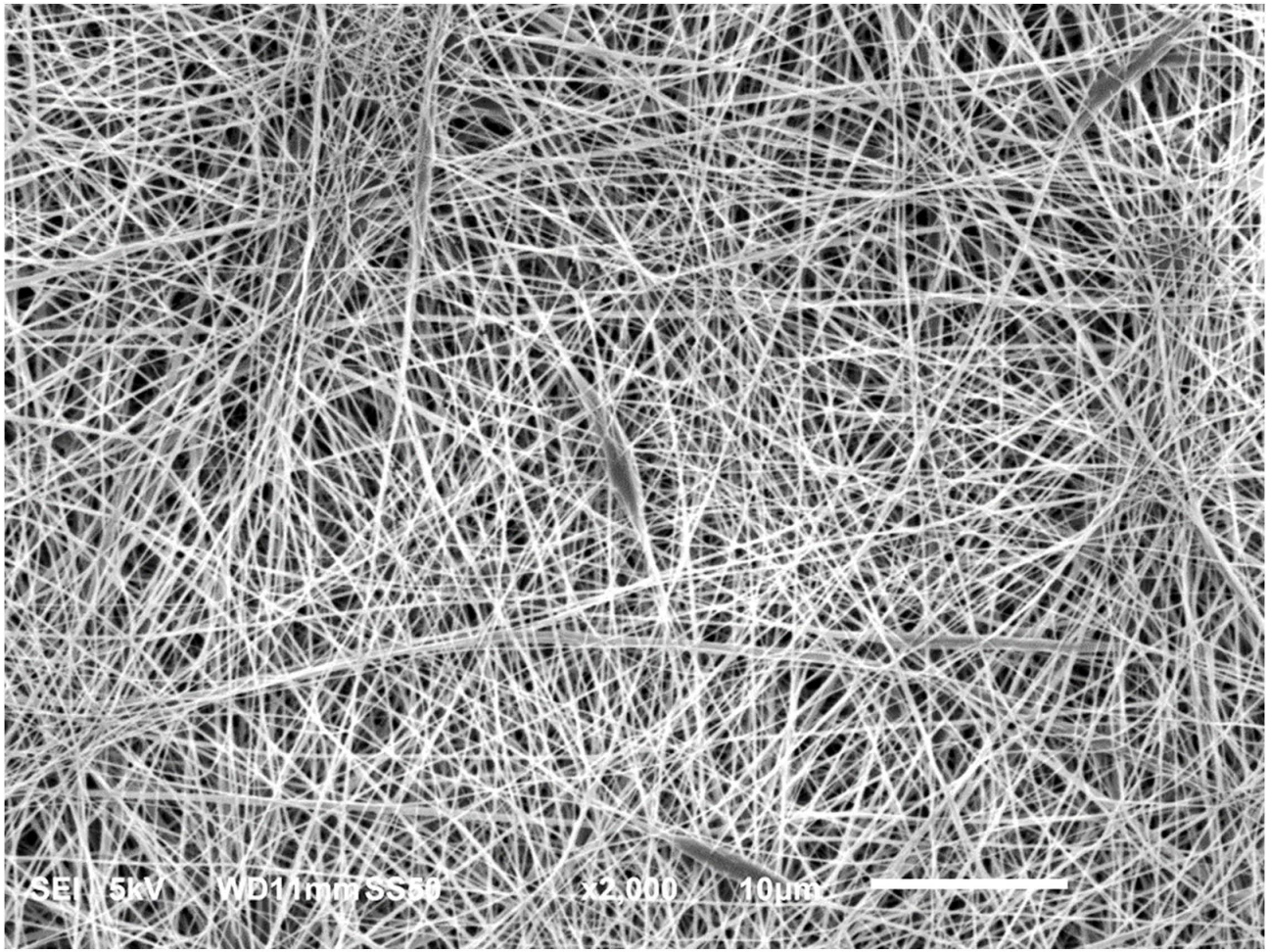

Supplementary Figure 5. Scanning electron microphotograph of BAPN-loaded PLGA nanofibers. Electrospinning results in a bulk, microporous scaffold comprised of individual nanofibers. Fibers were anisotropic with randomly oriented fibers. The darker, ballooning fibers are indicative of the presence of BAPN within the polymer matrix. Scale bar: 10 μm.